AIChE

Effects of Wood Biomass Type and Airflow Rate on Fuel and Soil Amendment Properties of Biochar Produced in a Top-Lit Updraft Gasifier

Hernán E. Díez and Juan F. Pérez

Grupo de Manejo Eficiente de la Energía (GIMEL), Departamento de Ingeniería Mecánica, Facultad de Ingeniería, Universidad de Antioquia, Medellín, Colombia; juanpb@udea.edu.co (for correspondence)

Published online 29 November 2018 in Wiley Online Library (wileyonlinelibrary.com). DOI 10.1002/ep.13105

In this study, the effects of biomass type and airflow rate on the fuel and soil amendment properties of a solid byproduct (biochar, BC) produced by gasification in a top-lit updraft reactor are studied. The results indicate that biomass with the highest fuel value index produces BC with the highest quality as a solid fuel. The best properties as a soil amendment are reached by Gua-30-BC as follows: the cation-exchange capacity (CEC) of 18.6 meq/100 g, the water holding capacity (WHC) of 438%, and the total oxidizable organic carbon (TOC) of 14.2%. When the airflow increases from 20 to 40 L/min, the properties of pine BC as a solid fuel are affected. An increase in the gasification temperature leads to a diminished bulk density. Moreover, the ash content increases affecting the heating value of BC, which decreases from 27.71 to 25.5 MJ/kg. The best properties of BC as a solid fuel are reached at 20 L/min. The properties of BC as a soil amendment are affected with increased airflow as follows: the CEC decreases by 22.8%, TOC increases by 232.3%, and WHC increases by 7.6%. The best properties of BC as a soil amendment are obtained at 40 L/min. © 2018 American Institute of Chemical Engineers Environ Prog, 38:e13105, 2019

Keywords: biochar, biomass gasification, solid byproduct, solid fuel, soil amendment

INTRODUCTION

Top-lit updraft (TLUD) gasifiers are used in the development of biomass cookstoves due to their relative simple design and low cost [1–3]. These reactors are also commonly used in laboratories for studying the downdraft biomass conversion in the fixed bed reverse mode. Such experimental setup allows analysis of the thermochemical processes of carbon-based materials under gasification (fuel-rich conditions) [4] and combustions regimes (fuel-lean conditions) [5] from an empirical point of view. The main stage of the conversion process is the pyrocombustion front, which is composed of the drying, pyrolysis, oxidation, and reduction sub-stages, moving from the reactor's top to bottom [6]. The biomass gasification process (fuel-rich conditions) leads to the production of a gaseous fuel (syngas) as well as biochar (BC) and tars as byproducts [6]. The gas yield depends on the reactor design or configuration. However, there are other variables (process parameters) that affect the gas yield such as biomass type, temperature, heating rate, pressure, residence time, catalyst, and others [7,8]. For biomass cookstoves, the main product is the producer gas for cooking meals [9], while biochar is a carbonaceous matrix byproduct that can be used for different applications such as energy or a soil amendment [10]. From the environmental point of view, biochar produced from biomass TLUD cookstoves can be used in the domestic context with the aim to contribute to sustainability. Therefore, it is important to understand the properties of biochar produced from a TLUD reactor and potential applications of this byproduct such as serving as a solid biofuel or a soil amendment [1,11,12].

Biochar can be used as a soil amendment to improve the soil quality of degraded lands due to anthropogenic and natural activities [13]. The soil quality parameters are water retention capability, electric conductivity, pH, and organic carbon. In addition, soil nutrients required by plants called essential nutrients, including macronutrients (C, H, O, N, P, K, S, Ca, and Mg) and micronutrients (B, Mn, Cu, Zn, Fe, Mo, and Mg) [13], can be supplied by biochar from TLUD cookstoves [10]. The cation-exchange capacity (CEC) is defined as the amount of exchangeable cations such as Ca^{2+}, Mg^{2+}, K^{+}, and NH_4^{+} that bound to a sample of soil [14].

Biochar produced from the thermochemical processes such as pyrolysis and gasification has advantages in comparison with compost because the natural decaying process of biochar is slower than that of compost [15]. This is a consequence of the high aromatic C structures of biochar that lead to a carbonaceous matrix to be more stable [16]. Therefore, studies that analyze the effect of biomass as a feedstock and airflow of the TLUD gasification process on properties of biochar as a solid fuel and a soil amendment are scant.

In the rural household context, biochar has also been proposed as a solid fuel due to its good properties such as a high heating value (>25 MJ/kg), a high fixed carbon level (>80 wt %), and a low moisture content (<5 wt %). Nevertheless, the heating value diminishes if the ash content of biochar increases [17,18]. Pacioni *et al.* [19] produced biochar from three agro-industry residues in a fixed bed reactor, concluding that biochar has the potential to generate energy through the gasification process mainly due to its high calorific value (>28 MJ/kg). Misinna and Rajabu [20] and Njenga *et al.* [17] obtained biochar derived from cookstoves (top lit updraft natural draft) and evaluated it by feeding back in TLUD cookstoves; the authors concluded that biochar as a fuel for cooking reduces the wood consumption by 40%–50%.

Different works that studied biochar produced from the thermochemical process (i.e., pyrolysis and gasification) as soil amendments are reported in the literature. Vaughn *et al.* [1] pyrolysed 13 wood species in a TLUD reactor to produce biochars for potential use in horticulture, highlighting that the majority of those wood species would be suitable for use in soil applications. Other works agree with the potential application of biochar in acid soils [21,22]. Another important property of biochar as soil amendment is the water holding capacity (WHC) that is favored by the formation of pores in biochar due to the release of the volatile matter [23,24].

In function of the literature cited, it is possible to find works that describe properties of biochar when used as a soil amendment. However, there is no consensus on the effect that gasification temperature has on CEC, which is one of the most important properties for a soil amendment [13]. In the literature, some studies reported that CEC increases with the gasification temperature [25], while others stated the contrary effect on CEC [26,27]. Thereby, the aim of this work is to study the effects of the feedstock (wood) type and primary airflow on biochars derived from the TLUD gasification process. The biochars samples have been characterized by proximate, ultimate and thermogravimetric analyses, bulk density, Fourier transform infrared spectroscopy (FTIR), scanning electron microscopy (SEM), surface area (Brebauer–Emmett–Teller [BET] method), CEC (meq/100 g), WHC, pH, and ash chemical composition. The results were focused to define potential applications for biochar in the rural context of TLUD gasifiers, because biomass TLUD cookstoves at a domiciliary scale produce a low amount of biochar that varies between 80 and 100 g per biomass kilogram [13,28].

MATERIALS AND METHODS

Biochar (BC) was produced using a laboratory scale TLUD reactor. The effect of feedstock on the BC characteristics was evaluated using four wood species from some representative Colombian regions. The selection and characterization of these biomasses are presented in detail by Díez and Pérez [29]. Furthermore, the effect of the airflow rate of gasification on BC properties was evaluated using *Pinus patula*. This feedstock was selected because it has the highest quality as a solid biofuel as quantified by the fuel value index (FVI, 9.89 MJ/cm^3) or energy density. The three rates of airflow analyzed were 20, 30, and 40 L/min. The primary airflow was supplied by a reciprocating compressor (2.6 kW at 3000 rpm, and 254 L/min) coupled with a plenum to absorb piston oscillations. Pressure and flow were regulated and measured by a manometer and a rotameter, respectively.

Wood Biomass Samples

The biomass species studied in this work are representative forest species from Colombia. The wood species are *Guazuma umlifolia*, Raw-Gua (from northern Colombia); *Cordia alliodora*, Raw-Nog (from northern Colombia); *Eucalyptus grandis*, Raw-Euc (from central Colombian); and *Pinus patula*, Raw-Pat (from southern Colombia). The samples were chipped under the same conditions (i.e., the engine speed and aperture of teeth) in a Bandit 95XP chipper; the chip sizes were between 4 and 20 mm. Samples were dried under the sunlight for 1 week, and then they were dried for 24 h at 103°C for characterization tests [29]. Table 1 shows the physical and chemical characteristics of the raw wood samples.

Experimental Setup

BCs were produced in an experimental facility with a TLUD gasifier at the laboratory scale (Figure 1) working at atmospheric pressure. The reactor mainly had an internal diameter of 102 mm, an external diameter of 185 mm, and a bed length of 400 mm. A description of the experimental setup is presented in detail in previous works [4,8,30]. The behavior of this reactor is similar to that of TLUD cookstoves operating only with primary air. Fresh biomass was ignited at the top, and the reaction front consisted of drying, pyrolysis, combustion, and reduction stages, going down until reaching the grate [2]. This reaction front is known as an autothermal pyrocombustion front [6,31]. Gasification parameters such as the biomass consumption rate, the maximum reaction temperature, and BC production can be obtained under controlled conditions. The obtained results can be extrapolated to improve the performance of gasifiers and TLUD cookstoves [8,28].

In relation to BCs produced, the effect of the feedstock type on biochar properties was evaluated using a fixed airflow rate of 30 L/min in the gasification process; the feedstock types were Raw-Gua, Raw-Nog, Raw-Euc, and Raw-Pat. Consequently, corresponding four BC samples from the raw species (Gua-30-BC, Nog-30-BC, Euc-30-BC, and Pat-30-BC) were obtained. During the BC production process, operating parameters of TLUD gasification were recorded, such as the flame front velocity (V_{ff}), the reaction temperature (T_{max}), the fuel-air equivalence ratio (F_{rel}), and the producer gas composition (Table 2). These gasification parameters may affect biochar properties [21,32]. In a similar way, these parameters were also recorded to analyze how the airflow rate affects properties of BCs using Raw-Pat species as feedstock. The three airflow rates were 20, 30, and 40 L/min. The effects of the feedstock type and airflow on the TLUD gasification process are presented in detail by Díez *et al.* [8].

Biochar Characterization

The mass yield of biochar is a term referred to the production of mass of biochar per kilogram of biomass, James *et al.* [28] estimated the biochar yield using Equation 1:

Table 1. Feedstock characterization (±standard deviation).

	Feedstock type			
	Raw-Gua	**Raw-Nog**	**Raw-Euc**	**Raw-Pat**
Proximate analysis (wt %)†				
Volatile matter	80.92	81.75	81.66	84.11
Fixed carbon	17.28	16.72	17.17	15.49
Ash	1.80	1.53	1.17	0.40
Moisture (wt %)	7.99	7.41	10.28	8.55
Ultimate Analysis (wt %)*				
C	49.1 (0.7)	49.2 (0.2)	51.0 (0.2)	47.2 (0.6)
H	5.8 (0.2)	5.8 (0.1)	6.1 (0.1)	6.2 (0.1)
N	n.d.	n.d.	n.d.	0.3 (0.01)
O**	45.1 (0.5)	45.0 (0.1)	42.9 (0.3)	46.3 (0.4)
Energy properties				
FVI (MJ/cm^3)	1.62 (0.03)	2.72 (0.05)	3.28 (0.08)	9.89 (0.26)
LHV_{db} (kJ/kg)	16,819 (91)	18,157 (38)	17,795 (90)	17,646 (143)
Physical properties				
Bulk density (kg/m^3)	138.26 (1.70)	169.70 (2.50)	221.83 (4.11)	196.42 (3.66)
Surface area (m^2/g)	2.1286	1.6960	1.7003	1.3489

Comments: Ultimate analysis (% w/w)
*daf, dry ash free basis.
**Oxygen estimated by difference.
†Proximate analysis on dry basis; n.d.: not detected.

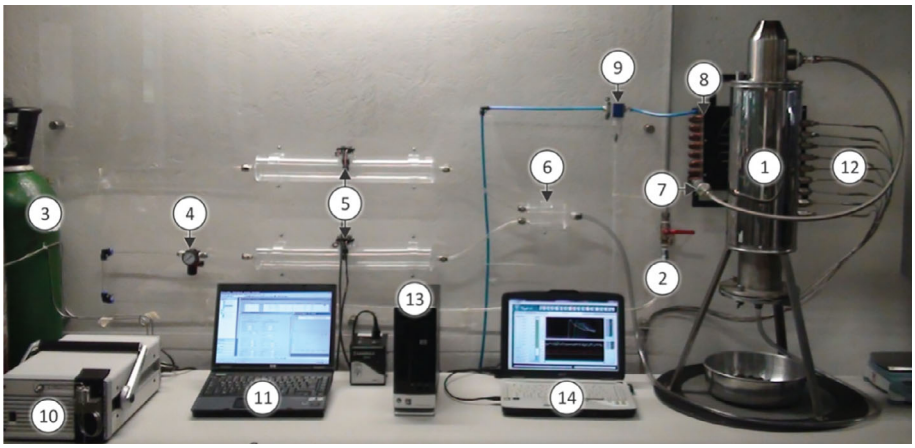

Figure 1. Picture of the experimental setup: (1) TLUD reactor, (2) Compressed air line, (3) Argon bottle for the chromatograph, (4) Pressure regulator, (5) Flow sensor, (6) Mixer, (7) and (8) Gas conditioning system, (9) Moisture condenser, (10) and (11) Gas chromatograph, (12) K-type thermocouples, (13) Data acquisition system, and (14) Computer for storage and display of data. [Color figure can be viewed at **wileyonlinelibrary.com**]

$$Y_{char,db} = \frac{m_{char} \times (1 - MC_{char} - Ash_{char})}{m_{fuel} \times (1 - MC_{fuel} - Ash_{fuel})} \quad (1)$$

where, m_{char} (kg) is the mass of biochar remaining from the TLUD gasification process, MC_{char} (kg) and Ash_{char} (kg) are the moisture and ash contents of biochar, respectively, m_{fuel} (kg) is the initial weight of wood (fuel), and MC_{fuel} (kg) and Ash_{fuel} (kg) are the moisture and ash contents of wood, respectively.

Physicochemical and Thermal Characterization

The proximate analysis of the wood samples was performed in a TGA-Q50 instrument according to the modified ASTM standard D5142-04 [33]. The ultimate analysis was carried out using the CHNSO (LECO) TruSpec Micro according to the ASTM D5373-08 method. Neither nitrogen (N) nor sulfur (S) was detected by the CHNSO (LECO) equipment in the wood samples analyzed in this study. The oxygen concentration (O) was estimated by difference [34]. Ash was produced at 600°C during 2 h to analyze its chemical composition, which was determined using an X-ray fluorescence thermo spectrometer (the Optim'X model).

The higher heating value (HHV) of biomass and the BC samples was measured in a calorimeter bomb (6100 Compensated jacket calorimeter) from Parr Instrument Company using the standard ASTM E144-14, HHV tests were conducted three times, and the low heating value (LHV) of the feedstocks and the BC samples was calculated based on HHV using Equation 2 [35].

$$LHV_{db} = HHV_{db} - 2260 \times M_{db} - 20300 \times H_{db} \quad (2)$$

where, HHV_{db} (kJ/kg) is the biomass higher heating value on the dry basis, M_{db} is the moisture content of the sample (g/g), and H_{db} is the hydrogen content (g/g) from the ultimate analysis.

The FVI quantifies the wood quality as a solid biofuel. Different models for estimating FVI have been proposed in the literature. Herein, FVI is defined as described by Cardoso *et al.* [36] according to Equation 3.

$$FVI = \frac{LHV_{db} \times \rho}{AC \times MC} \quad (3)$$

where, LHV_{db} is the lower heating value on the dry basis (MJ/kg), ρ is the biomass bulk density (kg/cm^3), and AC and MC are the ash content (g/g) and moisture content (g/g) of the sample, respectively. The bulk density was determined according to the procedure followed by Lenis *et al.* [37]. The test was replicated five times for each wood and BC sample.

Table 2. Gasification parameters for biochar production (±standard deviation).

Gasification parameters to produce wood biochars							
	Wood type effect				Airflow effect		
	Gua-30-BC	**Nog-30-BC**	**Euc-30-BC**	**Pat-30-BC**	**Pat-20-BC**	**Pat-30-BC**	**Pat-40-BC**
T_{max} (°C)	769.4 (36)	798.4 (45)	816.3 (39)	785.5 (53.3)	724.9 (31.5)	785.5 (53.3)	838.3 (47.1)
F_{rel} (−)	2.68 (0.24)	2.69 (0.15)	2.95 (0.2)	2.75 (0.24)	3.13 (0.20)	2.75 (0.24)	2.45 (0.16)
V_{ff} (mm/min)	14.8 (1.3)	12.1 (0.7)	9.5 (0.6)	11 (0.9)	7.9 (0.5)	11.0 (0.9)	12.3 (0.8)
Gas composition dry base (vol %)							
CO	11.5 (0.1)	11.7 (0.3)	12.9 (0.1)	12.3 (0.0)	12.9 (0.1)	12.3 (0.0)	11.3 (0.0)
CO_2	16.5 (0.3)	15.9 (0.2)	15.2 (0.4)	15.4 (0.1)	15.6 (0.1)	15.4 (0.1)	15.6 (0.2)
CH_4	1.7 (0.0)	1.7 (0.0)	1.6 (0.0)	1.6 (0.0)	1.8 (0.0)	1.6 (0.0)	1.3 (0.0)
H_2	7.1 (0.1)	7.3 (0.1)	6.0 (0.2)	6.1 (0.0)	5.7 (0.1)	6.1 (0.0)	6.0 (0.0)
N_2	63.2 (0.4)	63.4 (0.6)	64.3 (0.7)	64.6 (0.1)	64.0 (0.3)	64.6 (0.1)	65.8 (0.2)
Low heating value of producer gas (LHV_{pg}, MJ/Nm^3)							
LHV_{pg}	2.81 (0.02)	2.87 (0.02)	2.86 (0.05)	2.79 (0.01)	2.89 (0.02)	2.79 (0.01)	2.54 (0.01)

The FTIR spectroscopy for wood samples was carried out in a Fourier transform infrared spectrophotometer IRAffinity-1 (Shimadzu). The aim of this test was to identify functional groups of the biomass samples and their biochars [32,38]. The two main changes on the chemical surface structure of biochars identified by Fang *et al*. [39] are the dehydration and aromaticity. Thereby, in this work, the aromatic index was estimated as proposed by Brewer *et al*. [40] according to Equation 4:

$$A = \frac{FC}{FC + VM} \tag{4}$$

where, A is the aromaticity (dimensionless), FC is the fixed carbon (wt %), and VM is the volatile matter (wt %).

The thermogravimetric analysis (TGA) was conducted in a TG50 instrument. This test was carried out under the constant nitrogen flow (60 mL/min) from 25°C to 600°C at a heating rate of 10°C/min. Approximately 10 mg of each sample was used, which is similar to the method used by Poletto [41]. This test was used to analyze the thermal stability of the biochar samples with regards to the raw wood samples.

The surface area (BET) of the raw woods and the biochars were determined by gas adsorption isotherms using N_2 at −196°C as adsorptive with a Micrometrics ASAP 2020 equipment. The samples were outgassed to 80 μm Hg during 8 h. The BET theory was applied to the N_2 adsorption data in the interval relative pressure (P/P_o) of 0.06–0.3 at 77 K.

The changes in morphology of the cell wall structure of the woods and the biochars were observed using a scanning electron microscopy (SEM). Each sample (the wood species and their biochars) was covered with a gold film and placed in a JEOL JSM-6490 microscope, operating at an accelerating voltage of 30 kV in advance; the magnifications used for the analysis were ×500 and ×2000.

Biochar Characterization as a Soil Amendment

According to the NTC 5167 standard [42], a material for amending soils should satisfy the following conditions: total oxidizable organic carbon higher than 25%, maximum moisture content of approximately 20%, CEC higher than 30 meq/100 g, and heavy metalloid (As <41 ppm, Cd < 39 ppm, Cr < 1200 ppm, Hg < 17 ppm, Ni < 420 ppm, and Pb < 300 ppm). The CEC and organic carbon were determined according to the NTC 5167 standard. The moisture content was determined from the ultimate analysis according to the method used by Medic *et al*. [33], while the mineral composition was estimated by the X-ray fluorescence (XRF) analysis.

RESULTS AND DISCUSSION

Figure 2 shows the effect of the reaction temperature of the gasification process on the biochar production as a function of the feedstock type and airflows. If the reaction temperature increases, the production of biochar decreases because a high temperature favors the reaction mechanisms in the gasification process [43], which leads to the increase in the carbon conversion. In this study, the mass yield of biochar for all biomasses was between 8% and 11%. These results are similar to those presented by James *et al*. [44] who used a TLUD reactor at the laboratory scale and with the airflow rate of 20 L/min.

Biochar characterization as a solid fuel

Effect of the Feedstock Type

According to the ultimate analysis of biochar as a function of wood species (Gua-30-BC, Nog-30-BC, Euc-30-BC, and Pat-30-BC), these byproducts exhibited an increase in carbon content for up to approximately 81.06 wt % in dry and ash free basis, whereas the hydrogen and oxygen contents significantly decreased due to the devolatilization of biomass in the gasification process [45]. The higher mass concentration of the carbon content is consistent with the proximate analysis, where the fixed carbon also increased for the biochar samples; consequently, LHV of the biochar samples increased with regards to the raw woods. The ash content of the biochar samples affects their energy properties. It can be seen from Table 3 that the biochar samples with a higher ash content (~10 wt %), Gua-30-BC and Nog-30-BC, had a lower heating value (~23.3 MJ/kg) and FVI (~0.36 MJ/cm^3) than those of Pat-30-BC and Euc-30-BC (~27.5 and 3.57 MJ/cm^3 on average). On the other hand, the highest FVI (4.30 MJ/cm^3) of Pat-30-BC is attributed to its high LHV and its low ash content. However, when the obtained biochar samples were compared with the raw wood as a function of FVI, it was found that all studied biochar samples exhibited a significant reduction of this parameter. The low FVI value of the biochar samples is due to the decreasing bulk density and the increasing ash content (Equation 3). In spite of the biochar samples having a lower FVI value than that of the feedstocks, LHV of the BCs increased the potential of this solid byproduct to be used as a solid fuel [13,46].

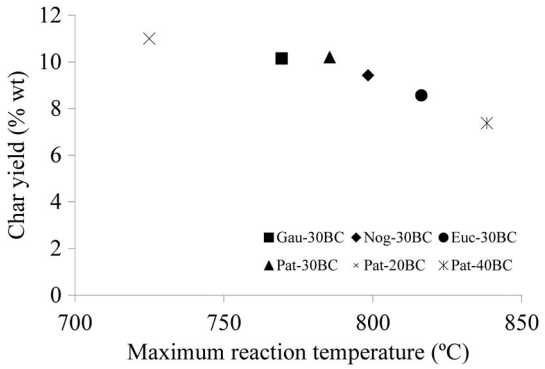

Figure 2. Effect of the maximum temperature measured inside the reactor on the mass yield of biochar as a function of the feedstock type and the airflow rate.

Considering that hemicellulose and cellulose were degraded in the gasification process (oxidative atmosphere) due to the high process temperature, the moisture content found in the biochars samples (Table 3) is attributed to the oxidation stage present in the pyrocombustion reaction front [47,48]. All biochar samples showed relatively low moisture content (<7.3%) despite the gasification temperatures exceeding the biomass drying temperatures (85°C–105°C). Therefore, the moisture could be produced by the condensation phenomena on a solid matrix as a product of volatiles and char oxidation reactions [49–51].

The mass loss during the process due to pyrocombustion reactions led to a diminishing bulk density of the biochars relative to the raw biomasses [52]. In addition, the release of volatiles led to an increase in the pore size on the surface leading to an increase in the surface area of the biochars. The pore structure and the surface area are important for determining the access of reactant gases to the internal surface area and active sites in the thermochemical conversion processes [53]. In this work, according to the feedstock type, when the reaction temperature increased from 769.4°C to 816.3°C, the surface area of the BC samples increased between 260.4 and 348.49 m^2/g.

Chemical Composition

The Van Krevelen diagram (Figure 3) allows for comparing raw wood samples with solid fossil fuels [54], and shows the position of biomass with regards to other fuels in terms of C, H, and O contents [55]. This position of biomass (solid fuel

Table 3. Biochar physicochemical characterization.

	Wood biochars						
	Feedstock type effect				Airflow effect		
	Gua-30	Nog-30	Euc-30	Pat-30	Pat-20	Pat-30	Pat-40
Proximate analysis d.b. (wt %)							
VM	11.96	13.20	7.23	14.25	16.55	14.25	11.46
FC	78.04	76.10	89.51	84.15	81.22	84.15	86.18
Ash	10.00	10.70	3.26	1.60	2.23	1.60	2.36
Aromatic index (–)	0.867	0.852	0.925	0.855	0.830	0.855	0.883
Moisture (wt %)	7.30	3.30	2.88	3.69	2.86	3.69	4.72
Ultimate analysis d.a.f. (wt %)							
C	87.57	83.40	75.72	82.92	81.67	82.92	81.91
H	0.47	0.60	0.87	0.21	1.39	0.21	0.47
O	9.94	15.99	23.39	16.83	16.91	16.83	17.59
N	2.02	0.01	0.02	0.04	0.03	0.04	0.03
S	n.d.	n.d.	n.d.	n.d.	n.d.	n.d.	n.d.
Energy properties							
$LHV_{d.b}$ (MJ/kg)	23.22	23.41	27.49	27.46	27.71	27.46	25.50
FVI (MJ/cm^3)	0.20	0.52	2.84	4.30	3.20	4.30	1.36
Physical properties							
BET (m^2/g)	260.40	298.86	348.49	318.32	258.93	318.32	431.78
Pore volume (cm^3/g)	0.0668	0.0578	0.0620	0.0488	0.0262	0.0488	0.1022
Bulk density (kg/m^3)	64.10	77.80	97.14	92.33	91.62	92.33	58.85

with low heating value) is due to the lower content of C and higher contents of H and O. However, all biochars produced show that H:C and O:C ratios significantly decreased by 80% and 90%, respectively. This is due to the loss of CH_3, CH_2 [56], and CO_2 caused by the gasification reactions leading to low H:C and O:C ratios in the BCs, thus increasing the C content in these solid byproducts [56].

With regards to the effect of the biomass type, the Van Krevelen diagram (Figure 3) shows that Gua-30-BC had the lowest O:C ratio, which indicates a low oxygen content with respect to the carbon content. This low ratio may be attributed to the fact that this raw species achieved the best gas quality in the gasification process due to its low hardness, low density, and high surface area, which favor the transfer of mass and energy in the thermochemical process [8]. The producer gas of Gua-30-BC exhibited the highest content of H_2 and CO compared with the other biomasses evaluated (Table 2). The opposite trend occurred with Euc-30-BC, which had high O:C and H:C ratios, because the high

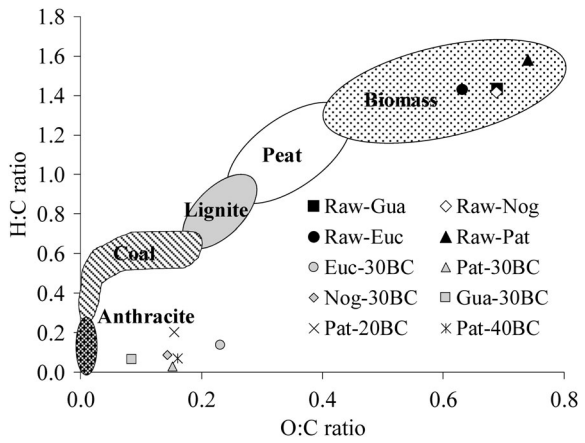

Figure 3. Van Krevelen diagram for raw biomasses and biochars as a function of the feedstock type and the airflow rate.

hardness of Raw-Euc hindered the diffusive processes of mass and energy transfer in the TLUD gasification.

TGA Analysis

Figure 4 shows that the four raw biomass samples have a similar behavior in terms of mass loss as a function of temperature. However, in the case of biochars, a large difference in thermal degradation can be observed (Figure 5). Weight loss from ambient temperature up to 150°C is associated with the release of moisture content present in biochar [57,58]. Thus, Gua-30-BC shows a high loss of mass at approximately 100°C, which is attributed to moisture losses and is congruent with the results from the proximate analysis (moisture content, 7.3 wt %). In the region between 200°C and 400°C, significant changes are not observed in the mass loss trends. Hemicellulose and cellulose decomposed in the gasification process, while a fraction of the lignin decomposed slightly from 500°C [59]. The gasification temperatures reached by the woods favored thermal degradation of the biomass components. However, in the case of Pat-20-BC, a small peak is observed at approximately 340°C, which is commonly attributed to the presence of cellulose [29]. This can be explained by the higher fuel–air equivalence ratio reached under this airflow rate (20 L/min); therefore, the gasification temperature is the lowest, and thus, a small fraction of cellulose could remain in the solid matrix of biochars.

The thermograms (Figure 5) show that all biochar samples have a high thermal stability due to the loss of some functional groups such as CH and OH (volatiles release). The biochar samples have similar mass loss values between 200°C and 400°C. In the range 400°C–600°C, all biochar samples continued to lose mass slightly; this is attributed mainly to the thermal degradation of the lignin, which decomposes slowly over a wide temperature range (160–900°C) [60,61]. This thermal stability associated with the solid byproducts gives biochars less reactive as solid fuels. Thereby, the fuel consumption using the biochars decreases due to their low kinetics rates [20].

FTIR Spectroscopy

In the FTIR, the main differences between the biochars and the raw biomasses are observed to be the dehydration and the

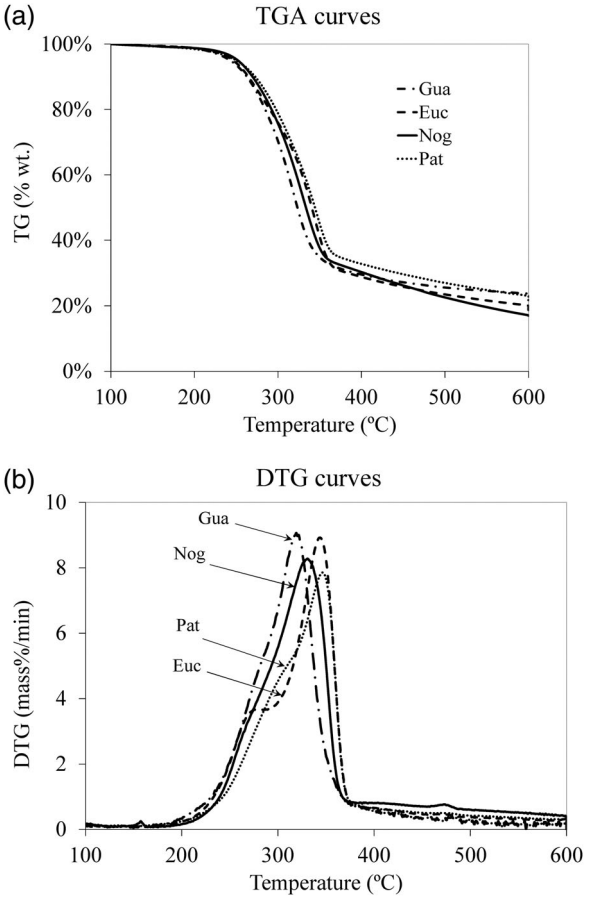

Figure 4. Thermal degradation of the four feedstock species (raw materials).

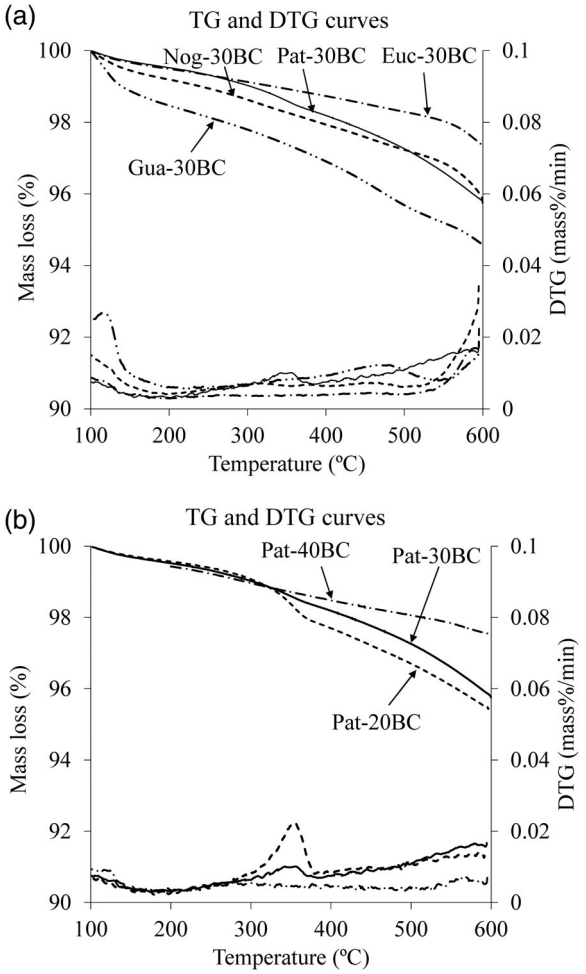

Figure 5. Thermal degradation of the biochar samples: (a) biochars derived from the different feedstock types, (b) biochars produced at the three airflow rates for Patula pine.

formation of aromatic structures. In Figure 6a, the region 3400–3200 cm^{-1} is associated with the O—H stretching [62], which is attributed to the moisture content or presence of hydroxyl or phenol groups [32]. The decrease of this peak is associated with the removal of moisture (dehydration) and volatile release processes. From the figure, the lowest presence of this functional group is in Euc-30-BC; this agrees with the proximate analysis, showing the lowest moisture content for this biochar (2.88 wt %). On the other hand, Gua-30-BC exhibits high intensity in this region, which is also consistent with the proximate analysis, showing the highest moisture content (7.3 wt %).

The region 2950–2800 cm^{-1} is associated with the aliphatic groups (CH_2 and CH_3) [63]. All biochars produced under the gasification regimes considered in this work show a significant reduction in the peaks between 2950 and 2800 cm^{-1}, which can be attributed to the enhancement of the aromatic structure of biochars by the thermal degradation of the hemicellulose and cellulose in the raw material [18]. The aliphatic structures from biomass might are destroyed by the release of volatiles in the TLUD gasification process [56]. These results agree with the ultimate analysis, which shows a decrease in H and O (Table 3), and the proximate analysis, which shows an increase in the fixed carbon of the biochars from 17% to 80% in relation to the raw materials. Moreover, the OH and CH bands (3400–3200 cm^{-1} and 2950–2800 cm^{-1}, respectively) are related to all constituents (cellulose, hemicellulose, and lignin); it is difficult to associate these changes to a particular constituent. However, the TLUD gasification process reaches temperatures higher than 700°C and solid residence times of 10–20 s [13,64]. Thereby, the high mass loss is due to the thermal decomposition of the hemicellulose and cellulose; this is in agreement with Figure 2, which shows the reduction of the H:C and O:C ratios due to devolatilization in the process.

Table 3 indicates that the Euc-30-BC has a higher aromaticity index, FC/(VM + FC); this agrees with Figure 6a, which shows that Euc-30-BC has a high loss of functional groups related to the CH and OH bands. In addition, Gua-30-BC shows a slight C—H stretching peak of approximately 3000 and 2800 cm^{-1}, which indicates a slight presence of the alkyl groups [32]. This functional group has a correlation with hydrophobicity; when alkyl (C—H) decreases, the hydrophobicity of the solid material increases [39].

The region between 2000 and 1600 cm^{-1} is an area with overtones and combination of bands; it means that it is not a reliable region in the FTIR results [65]. However, this region is commonly analyzed in biochars, especially 1800–1600 cm^{-1}, where the peaks associated with the aromatic C═O ring stretching and the C═C stretching of aromatic groups in lignin are present [45]. Nevertheless, it also can be attributed to the -OH in-plane bending modes, presence of water, and other common alkyl and oxygenated hydrocarbon functional groups [46], making it difficult to associate the peaks with functional groups. However, Figure 6a shows that the aromatic structure of the biochars is higher than that of the raw biomasses. The formation of an aromatic structure can be corroborated with the peak at 1420 cm^{-1} indicating the aromatic C—C ring

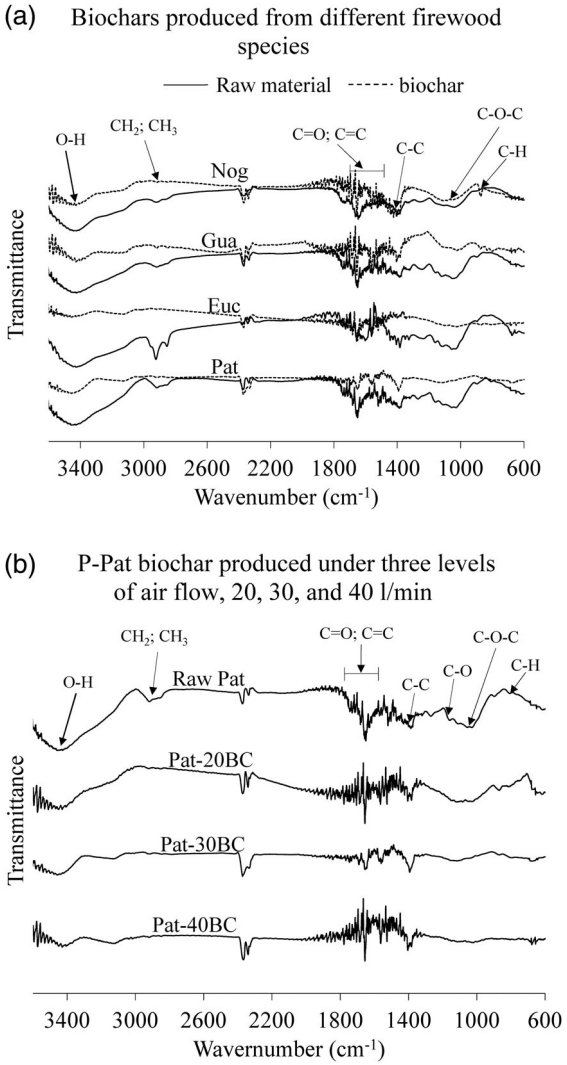

Figure 6. FTIR spectra for raw woods and biochar byproducts from TLUD biomass gasification as a function of the feedstock type and airflow.

stretching [47] and peaks within 850–780 cm^{-1}, associated with the aromatic C—H deformation [45]. At around 1200–1000 cm^{-1}, a peak associated with the C—O—C stretching in all feedstocks is observed due to the hemicellulose and cellulose contents [32]. However, this peak significantly decreases for the biochars because of the thermal degradation of the wood constituents (hemicellulose and cellulose) in the gasification process. Therefore, the solid matrix of the biochars has a higher lignin content, which is more thermally stable and whose heating value increases. These trends are also shown in the TGA behavior of the biochars.

SEM Analysis

The SEM images show that the four raw biomasses have different surface structures (Figure 7a, c, e, and g); Raw-Gua has a greater number of pores throughout the region where the image was recorded. Raw-Nog has a smaller number of pores than Raw-Gua; however, for both, the pores are closer than in the case of Raw-Euc and Raw-Pat (see white arrows in Figure 7c). Raw-Euc has a low porous surface, which can be attributed to its higher hardness, which results in more compact walls [66]. Raw-Pat has a surface with pores, but the pores are more separated than in the case of Raw-Gua and Raw-Nog.

Changes are observed on the surface of the biochars in relation to the raw biomass. In the case of Gua-30-BC and Nog-30-BC, the amount of pores increases due to the release of volatile matter in the gasification process. In addition, the presence of large pores can be observed in all biochars (see white arrows in Figure 7b, d, f, and h). While it can be seen that Euc-30-BC has a fibrous surface with few pores (the dotted white arrows indicating the presence of pores smaller than 5 μm), Gua-30-BC and Nog-30-BC have a large number of pores that are closer to each other.

By contrast, all biochars show the presence of agglomerated material on the surface (see white circles in Figure 7b, d, f, and h); this can be attributed to the tar recondensation on the BC surfaces and the inert material [67]. Euc-30-BC has less agglomerated material because it was produced at a higher temperature (816.3°C), which prevents the tar recondensation. Pat-30-BC has a higher presence of agglomerated material than Gua-30-BC and Nog-30-BC because Pat-30-BC has fewer pores on the surface, which makes the volatile matter release difficult, leading to the formation of a highly agglomerated material on its surface.

Effect of the Airflow Rate on Patula Pine Biochar

Physicochemical Properties

The physicochemical properties as a function of the airflow rate for Pat-20-BC, Pat-30-BC, and Pat-40-BC are shown in the column entitled "Airflow effect" in Table 3. The volatile matter of Pat-BC decreases between 16.55% and 11.46% as the airflow rate increases from 20 to 40 L/min. A high rate of airflow leads to a low fuel–air equivalence ratio, which means that the process slightly tends to combustion and thus the reaction temperature increases, favoring the release of the volatile matter (see Table 3). Thereby, the solid byproduct from the gasification process is a carbonaceous matrix with a high fixed carbon content, which increases from 81.22% to 86.18% as the airflow increases. Similarly, the carbon content increases when the airflow increases; this was analyzed in the chemical composition in Effect of the feedstock type section. In addition, a high release of the volatile matter leads to large size pores and a large surface area. On the other hand, Pat-40-BC has a high ash content because the oxidation reactions increases with increasing airflow. In all samples of Patula pine biochars, the reduction of moisture content of approximately 4% is evident. This low moisture content is associated with a higher process temperature that inhibits the moisture condensation on biochar surfaces [39].

In relation to the ultimate analysis, Raw-Pat has a lower carbon content (47.2%) than that of the produced biochars (>80%) in function of airflow (see Table 3). However, no significant difference is observed between the three values in function of airflow because the carbon content differs by only 1.6%; similarly, the oxygen content does not present a significant difference between the three BCs. On the other hand, the H content decreases as airflow increases, as shown in Table 3. Pat-20-BC has the highest hydrogen content of 1.39% in comparison with that of Pat-30-BC (0.21%) and Pat-40-BC (0.47%). Pat-40-BC and Pat-30-BC were produced at higher gasification temperatures compared with that of Pat-20-BC. Thus, as temperature increases, the breakdown of hydroxyl (O—H) and alkyl (C—H) functional groups is favored, which results in the reduction of the H content [14,18].

The Van Krevelen diagram (Figure 3) shows the reduction of the O:C and H:C ratios as airflow increases. A higher amount of air fed to the gasification process leads to the process to slightly tend to combustion. The increasing reaction temperatures favor the partial oxidation of the biomass main components (hemicellulose and cellulose), thus

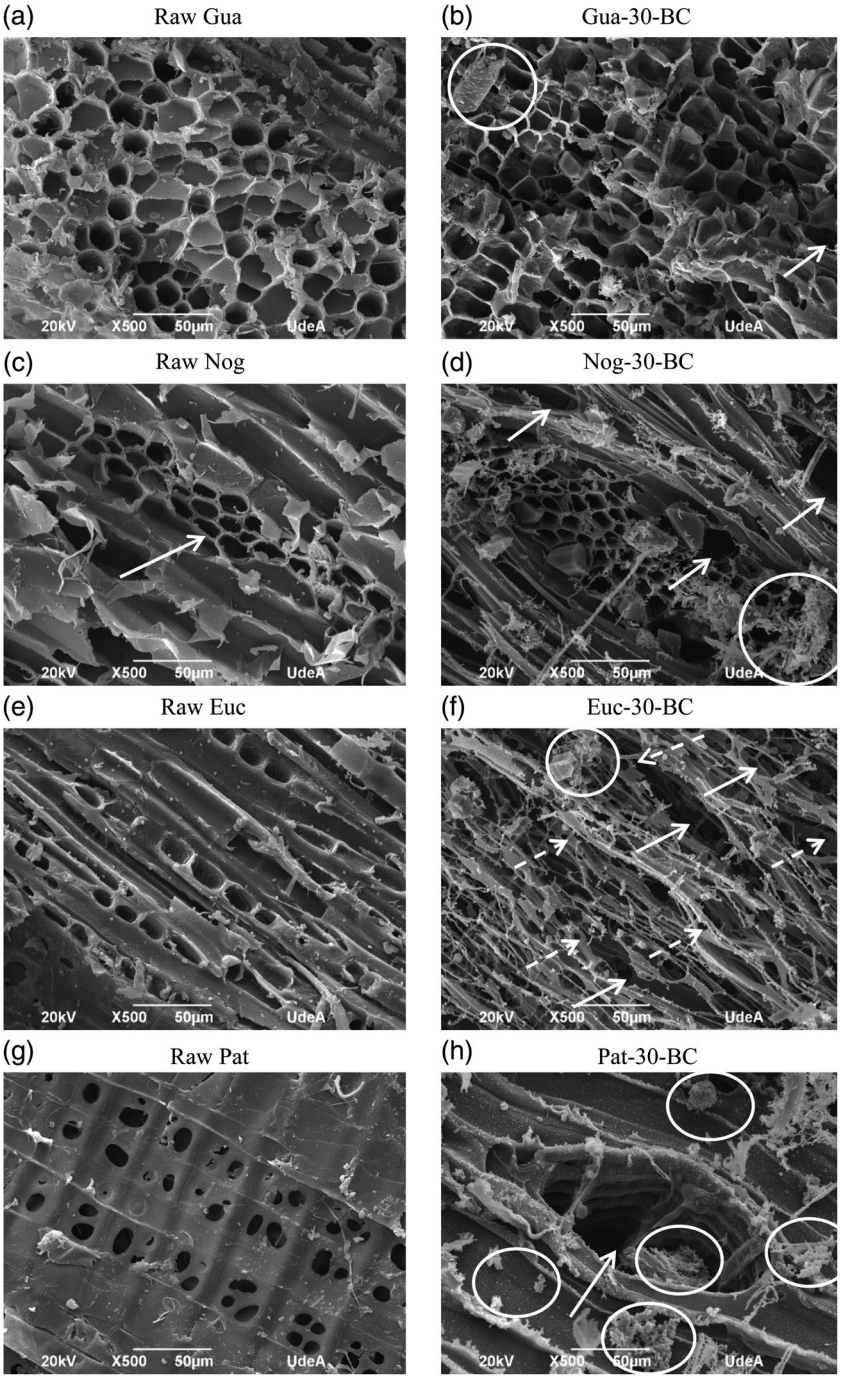

Figure 7. SEM images of biochar derived from the four feedstocks.

decreasing the content of oxygen and hydrogen in the biochars [28,50].

TGA Analysis

Figure 5b shows the biochars produced using different airflow rates (20, 30, and 40 L/min). In the thermograms, it is possible to see differences in the thermal stability of the biochars (Pat-20-BC, Pat-30-BC, and Pat-40-BC). As the air flow increases, the thermal degradation of the biochars decreases due to the fact that the process tends toward combustion; therefore, the gasification temperature is high, which increases the fixed carbon content in the biochars due to the oxidation of the biomass components [68]. Under these conditions of temperature and oxidative atmosphere, hemicellulose, cellulose, and a fraction of lignin of the biomass are expected to thermally degrade, resulting in a biochar rich in lignin, and a carbonaceous material with a heating value higher than the raw biomass. However, Pat-20-BC and Pat-30-BC show a slight peak between 300°C and 400°C. The peak of Pat-20-BC is higher than the peak of Pat-30-BC (see Figure 5b). These peaks can be attributed to the presence of a small fraction of cellulose in the two BC samples. In the case of Pat-40-BC, there is no evidence of a peak between 200°C and 400°C, due to the fact that the lower F_{rel} of gasification leads to a higher process temperature that favors the oxidation of the biomass components, mainly hemicellulose and cellulose. Between 400°C and 600°C, Pat-40-BC shows a thermal

stability higher than that of Pat-20-BC and Pat-30-BC because its higher reaction temperature favors its aromatic structure.

FTIR Analysis

Herein the effect of airflow on the changes in biochar functional groups with regards to the raw Patula pine biomass is analyzed. In the infrared spectrum (Figure 6b), a reduction in the peak between 3600 and 3200 cm^{-1} is observed. This peak is associated with the presence of the OH groups that refer to the moisture content or the presence of the hydroxyl or phenol group [14]. The peak between 3600 and 3200 cm^{-1} tends to diminish when the airflow increases. This trend is opposite to that of the moisture content of BCs, which increases with the airflow because the process slightly tends to combustion. Therefore, the temperature increases and the steam produced by the oxidation reactions increases; condensation of the steam on the BC surfaces is favored, leading to an increase in the moisture content of BCs as a function of airflow (Table 3). Then, the peak between 3600 and 3200 cm^{-1} decreases with airflow because the phenol groups diminish if the reaction temperature increases, which favors the thermal degradation of lignin from which phenols are derived [69].

The peaks in the region between 2900 and 2800 cm^{-1} decrease, which is attributed to the presence of alkyl (C—H stretching) [63]. In these bands, the spectrum of the biochars Pat-20-BC and Pat-30-BC presents a slight signal; nevertheless, Pat-40-BC does not have a signal in these bands. This is due to the higher reaction temperature (838.3°C) that favors the breakdown of these functional groups [39]. This result is consistent with the ultimate analysis, where the hydrogen content decreases from 1.39 to 0.47 wt %.

In Figure 6b, note that the biochars have a more aromatic structure than the raw biomass since the formation of an aromatic structure can be corroborated with the peak at 1420 cm^{-1}, indicating the aromatic C—C ring stretching [63,65]. In addition, as airflow increases, the peaks between 1000 and 1200 cm^{-1} decrease (associated with the C—O—C stretching of hemicellulose and cellulose). This behavior is attributed to the high gasification temperature that favors the release of volatiles associated with the biomass hemicellulose and cellulose [70].

SEM Analysis

In the TLUD gasifier where gases are released from the bottom to the top, the fuel–air equivalence ratio increases when airflow decreases; then, the reaction temperature decreases. Therefore, if the fuel–air equivalence ratio increases, the production of combustible gases concentration (molar fraction) and tars increases [71]. The agglomerated material on the biochar surface, shown in Figure 8b and c, is attributed to the recondensation reactions of tars on the biochar surfaces and some condensed mineral material [67]. The agglomerated or condensed material is more evident in the Pat-20-BC due to the high fuel–air equivalence ratio (F_{rel} = 2.9) reached under 20 L/min. Moreover, Pat-40-BC reached the highest reaction temperature; thus, recondensation or repolymerization of tars is inhibited. Therefore, the carbon matrix does not present this agglomerated material (Figure 8d). According to our results, the agglomerated material is observed mainly due to the tar condensation, because the reaction temperature increases at the highest rate of airflow and leads to the tar thermal cracking.

Similar results had been reported by Baliga *et al*. [72], who studied the structure of biochar from pyrolysis at 550°C, and found nanotubes on the biochar surfaces attributed to condensed volatiles on the hot biochars. Moreover, the agglomerated material on the biochar surface can be attributed to the formation of melt by the low thermal decomposition rate of the lignin [73,74].

The more evident condensed tar was observed for the lowest airflow rate of 20 L/min (SV_{air} = 0.042 m/s) due to the high tar concentration in the gas stream and the lowest reaction temperature. However, it does not mean that Pat-20-BC is the most aromatic biochar since the H:C ratio (0.2046) is higher than that of Pat-30-BC and Pat-40-BC. The aromatic structure of BC increases when the rate of airflow increases, which can be corroborated by the proximate analysis; Table 3 shows the increase of $FC/(FC + MV)$ with the airflow rate. Brewer [40]

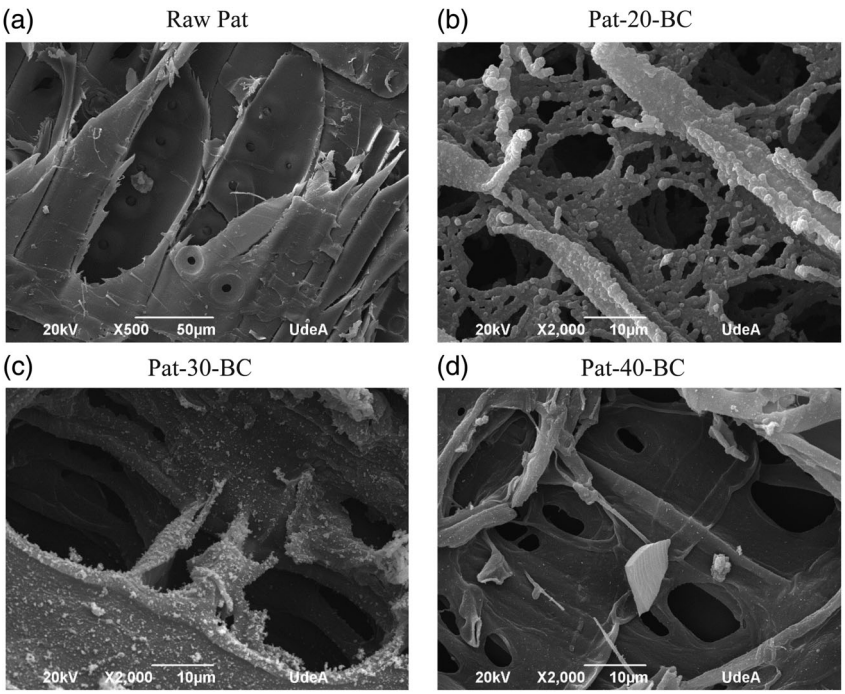

Figure 8. SEM images of biochar produced at three airflow rates (20, 30, and 40 L/min) for Patula pine.

Table 4. Mineral ash chemical composition of feedstock.

Mineral ash composition (%)	Raw-Gua	Raw-Nog	Raw-Euc	Raw-Pat
Na_2O	2.66	0.00	0.62	0.98
MgO	15.80	20.41	7.55	13.80
Al_2O_3	1.20	0.34	5.21	7.46
SiO_2	4.57	1.06	11.21	4.48
P_2O_5	16.70	3.66	5.25	9.45
SO_3	1.84	0.64	0.56	1.86
Cl	0.03	0.08	0.05	0.02
K_2O	3.43	0.08	3.36	2.11
CaO	51.21	71.62	53.34	54.51
TiO_2	0.00	0.00	0.41	0.00
Cr_2O_3	0.00	0.00	0.34	0.00
MnO	0.18	0.06	1.59	2.59
Fe_2O_3	1.51	0.65	9.44	2.23
NiO	0.10	0.25	0.55	0.09
CuO	0.26	0.09	0.07	0.17
SrO	0.43	0.95	0.19	0.22

stated that a high $FC/(FC + MV)$ ratio can be associated with a high level of aromaticity.

Biochar Properties as a Soil Amendment

Biochar is recognized in the literature as a potential soil amendment. Its properties such as CEC, WHC, TOC, density, surface area, electrical conductivity, nutrients, and mineral ash composition have been highlighted as soil improvers [13,32]. For instance, biochar has major positive effects on crop productivity when it is applied to acid soils [75].

At the rural household scale, biochar is an important reserve of soil nutrients; therefore, its application to soil amending is suggested because of its high mineral content of macronutrients (Ca, K, and P), and micronutrients (B, Mn, Cu, Zn, Fe, Mo, and Mg) [76].

Table 4 shows that Raw-Gua has the highest content of phosphorous (16.7%) in the ash; this chemical element is an essential macronutrient for plants [13]. However, Dume *et al.* [75] state that the phosphorous retention in acid soils requires the presence of iron and aluminium. Raw-Pat and Raw-Euc have a high amount of aluminium and iron, which could favor the retention of phosphorus in the soil. Herein, all studied ash compositions have a high Ca content, between 50% and 70%. Raw-Nog has the highest Ca content (70%) but it has the lowest K content. The plants require a high level of Ca, K, and P [76]. In conclusion, biochar has an ash content that is higher than that of raw biomass; therefore, the concentration of essential minerals for plants increases in biochar byproducts. This is one of the reasons why biochar is proposed for soil applications [13,77]. Other important properties of biochar for soil amendment are discussed below.

Effect of the Feedstock Type

TOC includes fractions of labile and recalcitrant. In biochars produced at high gasification temperatures (>700°C), the fraction of recalcitrant is expected to be high [13] since a high amount of the volatile material is released in the process. Regarding the produced biochars, Gua-30-BC and Nog-30-BC are the species with the highest carbon content as shown in the results of the ultimate analysis (Table 3). The raw species of Raw-Gua and Raw-Nog have a high surface area, which favors the diffusive processes of mass and heat transfer under the gasification regimes. This leads to a higher quality of the producer gas with a higher level of H_2 (7.1% and 7.3%, respectively). Such behaviour explains the high organic carbon content of these samples (Gua-30-BC and Nog-30-BC) that is associated with a low H content as the level of C increased in the remaining solid (biochars), see Table 3.

Another important property is WHC since crops can uptake water and nutrients [78]. All studied biochars present WHC higher than 300%. This property is favored by the pore formation and the surface area reached during the thermochemical process [79]. Gua-30-BC reached the highest WHC despite being the biochar with the smallest surface area (260.4 m^2/g). It has a large average pore volume (0.0668 cm^3/g), which favors WHC. In addition, as seen in the SEM images (Figure 7), Gua-30-BC and Nog-30-BC have the highest amount of pores.

Table 5. Biochar characterization as a soil amending.

	Biochar samples						
	Wood type effect				Air flow effect		
	Gua-30-BC	Nog-30-BC	Euc-30-BC	Pat-30-BC	Pat-20-BC	Pat-30-BC	Pat-40-BC
Properties as a soil amending							
Organic carbon (%)	14.2	15.3	9.33	8.25	3.22	8.25	10.7
Water holding capacity (%)	438	386	303	303	289	303	311
CEC (meq/100 g)	18.6	13.1	14.5	13.7	17.1	13.7	13.2
pH (10%)**	9.9	10.9	10.5	9.59	9.33	9.59	9.59
Electric conductivity* (dS/m)	0.0534	0.0421	0.017	0.0092	0.0063	0.0092	0.0124
Physical properties							
BET (m^2/g)	260.40	298.86	348.49	318.32	258.93	318.32	431.78
Pore volume (cm^3/g)	0.0668	0.0578	0.0620	0.0488	0.0262	0.0488	0.1022
Heavy metal(oid)s content							
As (ppm)	n.d.	n.d.	n.d.	n.d.	n.d.	n.d.	n.d.
Cd (ppm)	n.d.	n.d.	n.d.	n.d.	n.d.	n.d.	n.d.
Cr(ppm)	n.d.	n.d.	n.d.	n.d.	n.d.	n.d.	n.d.
Hg (ppm)	n.d.	n.d.	n.d.	n.d.	n.d.	n.d.	n.d.
Ni (ppm)	95.9	263.22	180.60	13.89	24.04	13.89	20.48
Pb (ppm)	n.d.	n.d.	n.d.	n.d.	n.d.	n.d.	n.d.

*Electric conductivity (1:200).
**pH (1:10); n.d.: not detected.

Thereby, it is possible to state that a high number of pores promotes WHC of biochars.

CEC is one of the biochar properties as a soil amendment that is highlighted in the literature [14,80,81] and is important in the processes of nutrition and plant growth [13]. The studied biochar has a high presence of minerals (Na, Mg, and K) that favors the increase of CEC [82] since the biochar has an ash content higher than that of the raw biomass (Tables 1 and 3). Table 5 shows that Gua-30-BC has the highest CEC; this is attributed to its high ash content (10 wt %) and its high mineral contents such as Na (2.66%), K (3.43%), and Mg (15.8%). On the other hand, although Nog-30-BC has the highest ash content, it does not have the highest CEC. This is attributed to the fact that it has less Na^+ and K^+ cations in the ash composition as shown in Table 4. Pat-30-BC has the lowest CEC due to its low ash content (1.60%), leading to a low concentration of minerals.

All biochars produced from gasification presented a pH level between 9.33 and 10.9. This result indicates that biochar could be suitable for improving acid soils since the alkaline nature of biochar exchanges H^+ with the soil. This exchange can contribute to increase of the soil pH level [83]. The pH levels of the biochar samples are in agreement with other works in the literature [21,75]. Biochar electrical conductivity is favored by the presence of the salts of sodium, potassium, magnesium, calcium, and carbonates. Gua-30-BC and Nog-30-BC have electrical conductivity higher than those of Euc-30-BC and Pat-30-BC. This is attributed to higher ash contents of Gua-30-BC and Nog-30-BC, by 10.0% and 10.7%, respectively. Therefore, our results suggest that the biochars can be used as a soil amendment in acid soils [21,75,83].

Effect of Airflow on Patula Pine Biochar

Total oxidizable organic carbon increases from 3.22% to 10.7% as the airflow rate increases from 20 to 40 L/min, which favors the release of the volatile matter producing a biochar with a high TOC due to its high aromaticity [13]. This behavior improves biochar characteristics as a soil amendment because the organic carbon from biochars leads to an increased soil organic carbon content [75]. This result is consistent with the proximate analysis since the content of the volatile matter decreased from 16.55% to 11.46%.

Table 5 shows that WHC increases with airflow. WHC improves due to a higher surface area and volume of pores favored by the volatile matter released at a higher gasification temperature [84].

CEC decreases from 17.1 meq/100 g to 13.2 meq/100 g as the airflow rate increases despite a higher surface area of the biochars with airflow. This behaviour is due to the fact that the gasification process temperature increases if the airflow rate supplied rises, which leads to a reduction of functional groups such as hydroxyl, carboxyl, and carbonyl [14]. A high presence of these functional groups favors chemical bonds with cations such as Na^+, K^+, and Mg^{2+} [26]. At the same time, the reduction of these functional groups during the gasification process leads to more stable (aromatic) structures, while Na^+, K^+, and Mg^{2+} cations form unions with the aromatic structure of the biochars through cation–π interactions leading to a decrease of CEC [12].

The studied biochars present properties as a soil amendment lower than suggested by technical Colombian standard (NTC 5761). The standard requires that a soil amendment meet the following requirements: CEC > 30 meq/100 g, organic carbon >25%, moisture content <20%, and the heavy metal content of As < 41 ppm, Cd < 39 ppm, Cr < 1200 ppm, Hg < 17 ppm, Ni < 420 ppm, and Pb < 300 pmm. Thus, not all biochars studied in this work fulfill the requirements for CEC and organic carbon parameters. These results suggest that the biochar produced from TLUD gasification could be used as a soil amendment, but the biochar requires treatments for improving its properties; for instance, mixing biochar and compost could be an excellent solution for rural sustainability [85]. Herein, the biochar samples characterized as a soil amendment require future research focusing on improving their properties to fulfill the NTC 5761 standard. Gaskin *et al.* [27] stated that post-production treatments for biochars are required to increase the immediate benefits of biochar on the soil for applications in agriculture. For example, mixing biochar with a soil amendment or fertilizer will improve CEC and organic carbon content [27].

CONCLUSIONS

The solid byproduct from biomass TLUD gasification, biochar, is suitable to be used as a solid fuel or as a soil amendment. In respect of the effect of the biomass type on biochar properties as a solid fuel, it was found that the biomass with the highest FVI produced the biochar with the highest FVI. Quality of this solid fuel increases from 0.2 to 4.3 MJ/cm^3 due to a low ash content (1.6 wt %) and a high heating value (27.46 MJ/kg) of Pat-30-BC. With regards to the effect of airflow on the properties of the Patula pine biochars as a solid fuel, it was found that the volatile matter decreases when the airflow rate increases, whereas fixed carbon and ash content tend to increase due to the high reaction temperature. The promoted thermal degradation of biomass constituents (hemicellulose and cellulose) with a high reaction temperature leads to a decrease in the bulk density of BCs. Therefore, the convergence of the high ash content and the low bulk density leads to a decrease in FVI and LHV (from 3.2 to 1.36 MJ/cm^3, and from 27.71 to 25.5 MJ/kg, respectively) as the airflow rate increases. Thus, the best properties of BC as a solid fuel are reached at 20 L/min due to the high reactivity, FVI, and LHV.

The presence of macronutrients and micronutrients in biochar and properties such as CEC, TOC, and WHC suggest the suitability of BCs for soil amendment applications. For the effect of biomass, it was found that the formation of pores in the produced biochar favors WHC. By contrast, as the reaction temperature increases, CEC decreases because of the loss of functional groups such as hydroxyl, carboxyl and carbonyl due to the thermal degradation of biomass constituents (hemicellulose and cellulose), which confers a high aromaticity index (stable) and a high surface area (BET) to the biochars. In relation to the effect of feedstock on soil amendment properties of the BCs, Gua-30-BC is highlighted as the BC with the best properties as a soil amendment due to the highest CEC (18.6 meq/100 g), high WHC (438%), and TOC (14.2%). If the airflow rate increases, TOC increases from 3.22% to 10.7%, WHC increases from 289% to 311%, and surface area increases from 258.93 to 431.78 m^2/g. These properties are important in a soil amendment. However, CEC decreases (from 17.1 meq/100 g to 13.2 meq/100 g) as the airflow rate increases. Therefore, the best biochar properties as a soil amendment are obtained at 40 L/min due to the highest surface area, WHC, and TOC. Further studies are required to improve the properties of BCs as a soil amendment.

ACKNOWLEDGMENTS

The authors acknowledge the financial support of CODI-Universidad de Antioquia through the research project "Energy evaluation and emissions of an eco-efficient cookstove based on biomass micro-gasification at household scale (in Spanish) - PRG2017-16230".

LITERATURE CITED

1. Vaughn, S., Kenar, J., Eller, F., Moser, B., Jackson, M., & Peterson, S. (2015). Physical and chemical characterization of biochars produced from coppiced wood of thirteen tree species for use in horticultural substrates, Industrial Crops and Products, 66, 44–51.

2. Tryner, J., Willson, B., & Marchese, A. (2014). The effects of fuel type and stove design on emissions and efficiency of natural-draft semi-gasifier biomass cookstoves, Energy for Sustainable Development, 23, 99–109.
3. Jetter, J., Zhao, Y., Smith, K., Khan, B., Yelverton, T., Decarlo, P., et al. (2012). Pollutant emissions and energy efficiency under controlled conditions for household biomass cookstoves and implications for metrics useful in setting international test standards, Environmental Science & Technology, 46, 10827–10834.
4. González, W.A., Pérez, J.F., Chapela, S., & Porteiro, J. (2018). Numerical analysis of wood biomass packing factor in a fixed-bed gasification process, Renewable Energy, 121, 579–589.
5. Kirch, T., Medwell, P.R., & Birzer, C.H. (2016). Natural draft and forced primary air combustion properties of a top-lit up-draft research furnace, Biomass and Bioenergy, 91, 108–115.
6. Pérez, J.F., Benjumea, P.N., & Melgar, A. (2015). Sensitivity analysis of a biomass gasification model in fixed bed downdraft reactors: effect of model and process parameters on reaction front, Biomass and Bioenergy, 83, 403–421.
7. Pérez, J.F., Melgar, A., & Benjumea, P.N. (2012). Effect of operating and design parameters on the gasification/combustion process of waste biomass in fixed bed downdraft reactors: an experimental study, Fuel, 96, 487–496.
8. Díez, E., Gómez, I.N., & Pérez, J.F. (2018). Mass, energy, and exergy analysis of top-lit updraft micro-gasification process: effect of firewood type and forced primary airflow, Sustainable Energy Technologies and Assessments, 29, 82–91.
9. Njenga, M., Iiyama, M., Jamnadass, R., Helander, H., Larsson, L., de Leeuw, J., Neufeldt, H., Röing De Nowina, K., & Sundberg, C. (2016). Gasifier as a cleaner cooking system in rural Kenya, Journal of Cleaner Production, 121, 208–217.
10. Birzer, C., Medwell, P., MacFarlane, G., Read, M., Wilkey, J., Higgins, M., & West, T. (2014). A Biochar-producing, dung-burning cookstove for humanitarian purposes, Procedia Engineering, 78, 243–249.
11. Hagner, M., Hallman, S., Jauhiainen, L., Kemppainen, R., Rämö, S., Tiilikkala, K., & Setälä, H. (2015). Birch (Betula spp.) wood biochar is a potential soil amendment to reduce glyphosate leaching in agricultural soils, Journal of Environmental Management, 164, 46–52.
12. Ladygina, N., & Rineau, F. (2013). Biochar and soil biota: the potential of biochar amendments to remediate contaminated soils, Boca Raton: CRC Press, Taylor & Francis Group.
13. Ok, Y., Uchimiya, S., Chang, S., & Bolan, N. (2016). Biochar: production, characterization, and applications, New York: CRC Press, Taylor & Francis Group.
14. Leeq, J., Kidder, M., Evans, B., Paik, S., Buchanan, A., Garteh, C., et al. (2010). Characterization of biochars produced from cornstovers for soil amendment, Environmental Science & Technology, 44, 1970–1974.
15. Steiner, C. (2017). Las perspectivas de biocarbón: secuestro de carbono, ciclo de nutrientes y generación de energía, Revista Palmas, 31, 116–125.
16. Raya-Moreno, I., Cañizares, R., Domene, X., Carabassa, V., & Alcañiz, J.M. (2017). Comparing current chemical methods to assess biochar organic carbon in a Mediterranean agricultural soil amended with two different biochars, Science of the Total Environment, 598, 604–618.
17. Njenga, M., Mahmoud, Y., Mendum, R., Iiyama, M., Jamnadass, R., Roing De Nowina, K., et al. (2017). Quality of charcoal produced using micro gasification and how the new cook stove works in rural Kenya, Environmental Research Letters, 12, 1–12.
18. Pehlivan, E., Özbay, N., Yargıç, A.S., & Şahin, R.Z. (2017). Production and characterization of chars from cherry pulp via pyrolysis, Journal of Environmental Management, 203, 1017–1025.
19. Pacioni, T.R., Soares, D., Domenico, M., Rosa, M.F., Moreira, R., & José, H.J. (2016). Bio-syngas production from agro-industrial biomass residues by steam gasification, Waste Management, 58, 221–229.
20. Misginna, M.T., & Rajabu, H.M. (2014). The Potential of charcoal making stove to enhance energy efficiency, International Journal of Innovation and Applied Studies, 5, 206–214.
21. Dume, B., Berechar, G., & Tulu, S. (2015). Characterization of biochar produced at different temperatures and its effect on acidic nitosol of jimma, southwest Ethiopia, International Journal of Soil Science, 10, 63–73.
22. Trippe, K.M., Griffith, S.M., Banowetz, G.M., & Whitaker, G.W. (2015). Changes in soil chemistry following wood and grass biochar amendments to an acidic agricultural production soil, Agronomy Journal, 107, 1440–1446.
23. Novak, J., Lima, I., Xing, B., Gaskin, J., Steiner, C., Das, K. C., et al. (2009). Characterization of designer biochar produced at different temperatures and their effects on a loamy sand, International Journal of the Environmental Sciences, 3, 195–206.
24. Shafie, S., Amran Mohd, M., Hang, L.L., Mukhlesur, M., & Wan Ab Karim Ghani, W.A. (2012). Effect of pyrolysis temperature on the biochar nutrient and water retention capacity, Journal of Purity, Utility Reaction and Environment, 1, 323–337.
25. Ashworth, A., Sadaka, S., Allen, F., Sharara, M., & Keyser, P. (2014). Influence of pyrolysis temperature and production conditions on switchgrass biochar for use as a soil amendment, BioResources, 9, 7622–7635.
26. Sizmur, T., Quiliam, R., Puga, A., Moreno-Jiménez, E., Beesley, L., & Gomez-Eyles, J. (2016). Agricultural and environmental applications of biochar: advances and barriers, Soil Science Society of America, 63, 495–504.
27. Gaskin, J., Steiner, C., Harris, K., Das, K.C., & Bibens, B. (2008). Effect of low-temperature pyrolysis conditions on biochar for agricultural use, Transactions of the ASABE, 51, 2061–2069.
28. James, R., Yuan, W., & Boyette, D.M. (2016). The effect of biomass physical properties on top-lit updraft gasification of woodchips, Energies, 9, 283.
29. Díez, H., & Pérez, J.F. (2017). Physicochemical characterization of representative firewood species used for cooking in some Colombian regions, International Journal of Chemical Engineering, 2017, 1–13.
30. Lenis, Y.A., Agudelo, A.F., & Pérez, J.F. (2013). Analysis of statistical repeatability of a fixed bed downdraft biomass gasification facility, Applied Thermal Engineering, 51, 1006–1016.
31. Pérez, J.F., Melgar, A., & Tinaut, F.V. (2014). Modeling of fixed bed downdraft biomass gasification: application on lab-scale and industrial reactors, International Journal of Energy Research, 38, 319–338.
32. Qian, K., Kumar, A., Patil, K., Bellmer, D., Wang, D., Yuan, W., & Huhnke, R. (2013). Effects of biomass feedstocks and gasification conditions on the physiochemical properties of char, Energies, 6, 3972–3986.
33. Medic, D., Darr, M., Shah, A., Potter, B., & Zimmerman, J. (2012). Effects of torrefaction process parameters on biomass feedstock upgrading, Fuel, 91, 147–154.
34. Protásio, T., Bufalino, L., Tonoli, G., Guimarães, M., Trugilho, P.F., & Mendes, L.M. (2013). Brazilian lignocellulosic wastes for bioenergy production: characterization and comparison with fossil fuels, BioResources, 8, 1166–1185.

35. Cheng, J. (2009). Biomass to renewable energy processes, Boca Raton: CRC Press, Taylor & Francis Group.
36. Cardoso, M.B., Ladio, A.H., Dutrus, S.M., & Lozada, M. (2015). Preference and calorific value of fuel wood species in rural populations in northwestern Patagonia, Biomass and Bioenergy, 81, 514–420.
37. Lenis, Y.A., Pérez, J.F., & Melgar, A. (2016). Fixed bed gasification of Jacaranda Copaia wood: effect of packing factor and oxygen enriched air, Industrial Crops and Products, 84, 166–175.
38. Popescu, M., Popescu, C., Lisa, G., & Sakata, Y. (2011). Evaluation of morphological and chemical aspects of different wood species by spectroscopy and thermal methods, Journal of Molecular Structure, 988, 65–72.
39. Fang, Q., Chen, B., Lin, Y., & Guan, Y. (2013). Aromatic and hydrophobic surfaces of wood-derived biochar enhance perchlorate adsorption via hydrogen bonding to oxygen-containing organic groups, Environmental Science & Technology, 48, 279–288.
40. Brewer, C.E., Unger, R., Schmidt-Rohr, K., & Brown, R.C. (2011). Criteria to select biochars for field studies based on biochar chemical properties, Bioenergy Research, 4, 313–323.
41. Poletto, M. (2016). Effect of extractive content on the thermal stability of two wood species from Brazil, MADERAS: Ciencias y Tecnología, 18, 435–442.
42. Instituto Colombiano de Normas Técnicas (NTC). Productos para la industria agrícola. Productos orgánicos usados como abonos o fertilizantes y enmiendas de suelo - NTC 5167 Standard, 2011, 1–58.
43. Protásio, T., Melo, I., Guimarães, M., Mendes, R.F., & Trugilho, P.F. (2013). Thermal decomposition of torrefied and carbonized briquettes of residues from coffee grain processing, Ciência e Agrotecnologia, 37, 221–228.
44. James, R., Yuan, W., Boyette, D.M., & Wang, D. (2015). The effect of air flow rate and biomass type on the performance of an updraft biomass gasifier, BioResources, 10, 3615–3624.
45. Jindo, K., Mizumoto, H., Sawada, Y., Sanchez-Monedero, M., & Sonoki, T. (2014). Physical and chemical characterization of biochars derived from different agricultural residues, Biogeosciences, 11, 6613–6621.
46. Qian, K., Kumar, A., Bellmer, D., Yuan, W., Wang, D., & Eastman, M.A. (2015). Physical properties and reactivity of char obtained from downdraft gasification of sorghum and eastern red cedar, Fuel, 143, 383–389.
47. Kausley, S.B., & Pandit, A.B. (2010). Modelling of solid fuel stoves, Fuel, 89, 782–791.
48. Porteiro, J., Patiño, D., Collazo, J., Granada, E., Moran, J., & Miguez, J.L. (2010). Experimental analysis of the ignition front propagation of several biomass fuels in a fixed-bed combustor, Fuel, 89, 26–35.
49. Font Palma, C. (2013). Modelling of tar formation and evolution for biomass gasification: a review, Applied Energy, 111, 129–141.
50. Tinaut, F.V., Melgar, A., Pérez, J.F., & Horrillo, A. (2008). Effect of biomass particle size and air superficial velocity on the gasification process in a downdraft fixed bed gasifier. An experimental and modelling study, Fuel Processing Technology, 89, 1076–1089.
51. Sadaka, S., Sharara, A.M., Ashworth, A., Keyser, P., Allen, F., & Wright, A. (2014). Characterization of biochar from switchgrass carbonization, Energies, 7, 548–567.
52. Martínez, J.D., Murillo, R., García, T., & Arauzo, I. (2014). Thermodynamic analysis for syngas production from volatiles released in waste tire pyrolysis, Energy Conversion and Management, 81, 338–353.
53. Qian, L., Zhao, Y., Sun, S., Che, H., Chen, H., & Wang, D. (2014). Chemical/physical properties of char during devolatilization in inert and reducing conditions, Fuel Processing Technology, 118, 327–334.
54. McKendry, P. (2002). Energy production from biomass (part 2): conversion technologies, Bioresource Technology, 83, 47–54.
55. Janajreh, I., & Al Shrah, M. (2013). Numerical and experimental investigation of downdraft gasification of wood chips, Energy Conversion and Management, 65, 783–792.
56. Wiedner, K., Rumpel, C., Steiner, C., Pozzi, A., Maas, R., & Glaser, B. (2013). Chemical evaluation of chars produced by thermochemical conversion (gasification, pyrolysis and hydrothermal carbonization) of agro-industrial biomass on a commercial scale, Biomass and Bioenergy, 59, 264–278.
57. Sellin, N., Krohl, D.R., Marangoni, C., & Souza, O. (2016). Oxidative fast pyrolysis of banana leaves in fluidized bed reactor, Renewable Energy, 96, 56–64.
58. Cárdenas-Aguiar, E., Gascó, G., Paz-Ferreiro, J., & Méndez, A. (2017). The effect of biochar and compost from urban organic waste on plant biomass and properties of an artificially copper polluted soil, International Biodeterioration & Biodegradation, 124, 223–232.
59. Mašek, O. (2016). Biochar in thermal and thermochemical biorefineries-production of biochar as a coproduct. In R. Luque, C. Lin, K. Wilson, & J. Clark (Eds.), Handbook of biofuels production. (2nd Edition, pp. 655–671), New York: Elsevier.
60. Kumar, D., & Pant, K.K. (2015). Production and characterization of biocrude and biochar obtained from non-edible de-oiled seed cakes hydrothermal conversion, Journal of Analytical and Applied Pyrolysis, 115, 77–86.
61. Arteaga-Pérez, L.E., Segura, C., Bustamante-García, V., Cápiro, G.O., & Jiménez, R. (2015). Torrefaction of wood and bark from Eucalyptus globulus and *Eucalyptus nitens*: focus on volatile evolution *vs* feasible temperatures, Energy, 93, 1731–1741.
62. Naik, S., Goud, V., Rout, P.K., Jacobson, K., & Dalai, A.K. (2010). Characterization of Canadian biomass for alternative renewable biofuel, Renewable Energy, 35, 1624–1631.
63. Liu, Q., Zhong, Z., Wang, S., & Luo, Z. (2013). Interactions of biomass components during pyrolysis: a TG-FTIR study, Journal of Analytical and Applied Pyrolysis, 90, 213–908.
64. Mohseni, M., Peters, B., & Baniasadi, M. (2017). Conversion analysis of a cylindrical biomass particle with a DEM-CFD coupling approach, Case Studies in Thermal Engineering, 10, 343–356.65.
65. Allen, R.M., & Laird, D.A. (2013). Quantitative prediction of biochar soil amendments by near-infrared reflectance spectroscopy, Soil Science Society of America Journal, 77, 1784–1794.
66. Chen, H. (2014). Chemical composition and structure of natural lignocellulose. In H. Chen (Ed.), Biotechnology of lignocellulose: theory and practice. (pp. 25–71), Dordrecht: Springer Netherlands.
67. Fryda, L., & Visser, R. (2015). Biochar for soil improvement: evaluation of biochar from gasification and slow pyrolysis, Agriculture, 5, 1076–1115.
68. Bhaskar, T., Bhavya, B., Singh, R., Naik, D.V., Kumar, A., & Goyal, H.B. (2011). Chapter 3 – Thermochemical conversion of biomass to biofuels. In A. Pandey, C. Larroche, S.C. Ricke, C.-G. Dussap, & E. Gnansounou (Eds.), Biofuels. (pp. 51–77), New York: Academic Press.
69. Pérez, J.F., Pelaez-Samaniego, M.R., & Garcia-Perez, M. (2017). Torrefaction of fast-growing Colombian wood species, Waste and Biomass Valorization, 102, 1–13.
70. Kumar, A., Jones, D., & Milforf, H. (2009). Thermochemical biomass gasification: a review of the current status of the technology, Energies, 2, 556–581.
71. Devi, L., Ptasinski, K.J., & Janssen, F. (2003). A review of the primary measures for tar elimination in biomass gasification processes, Biomass and Bioenergy, 24, 125–140.
72. Baliga, V., Sharma, R., Miser, D., McGrath, T., & Hajaligol, M. (2003). Physical characterization of pyrolyzed

tobacco and tobacco components, Journal of Analytical and Applied Pyrolysis, 66, 191–215.
73. Sharma, R.K., Wooten, J.B., Baliga, V.L., Lin, X., Geoffrey Chan, W., & Hajaligol, M.R. (2004). Characterization of chars from pyrolysis of lignin, Fuel, 83, 1469–1482.
74. Pelaez-Samaniego, M.R., Yadama, V., Garcia-Perez, M., Lowell, E., & McDonald, A.G. (2014). Effect of temperature during wood torrefaction on the formation of lignin liquid intermediates, Journal of Analytical and Applied Pyrolysis, 109, 222–233.
75. Dume, B., Ayele, D., Regassa, A., & Barecha, G. (2017). Improving available phosphorus in acidic soil using biochar, Journal of Soil Science and Environmental Management, 8, 87–94.
76. Baptista, I., Miranda, I., Quilhó, T., Gominho, J., & Pereira, H. (2013). Characterization and fractioning of *Tectona grandis* bark in view of its valorization as a biorefinery raw-material, Industrial Crops and Products, 50, 166–175.
77. Yao, D., Hu, Q., Wang, D., Yang, H., Wu, C., Wang, X., & Chen, H. (2016). Hydrogen production from biomass gasification using biochar as a catalyst/support, Bioresource Technology, 216, 159–164.
78. Yu, O., Harper, M., Hoepfl, M., & Domermuth, D. (2017). Characterization of biochar and its effect on the water holding of loamy sand soil: comparison of hemlock biochar and switchblade grass biochar characteristics, Environmental Progress & Sustainable Energy, 0, 1–6.
79. Ghani, W., Mohd, A., da Silva, G., Bachmann, R.T., Taufiq-Yap, Y.H., Rashid, U., et al. (2013). Biochar production from waste rubber-wood-sawdust and its potential use in C sequestration: chemical and physical characterization, Industrial Crops and Products, 44, 18–24.
80. Wu, W., Yang, M., Feng, Q., McGrouther, K., Wang, H., Lu, H., & Chen, Y. (2012). Chemical characterization of rice straw-derived biochar for soil amendment, Biomass and Bioenergy, 47, 268–276.
81. Mia, S., Uddin, N., Mamum Hossain, S.A., Al, Amin, R., METE, F., & Hiemstra, T. (2015). Production of biochar for soil application: a comparative study of three kiln models, Pedosphere, 25, 696–702.
82. Senior, E. (1995). Microbiology of landfill sites. (2nd Edition), Boca Raton: CRC Press, Taylor & Francis Group.
83. Streubel, J., Collins, H., Garcia-Perez, M., Tarara, J., Granatstein, D., & Kruger, C. (2011). Influence of contrasting biochar types on five soils at increasing rates of application, Soil Science Society of America Journal, 75, 1402–1413.
84. Brewer, C.E., Schmidt-Rohr, K., Satrio, J., & Brown, R.C. (2009). Characterization of biochar from fast pyrolysis and gasification systems, Environmental Progress & Sustainable Energy, 28, 386–396.
85. Kisiki-Nsamba, H., Hale, S.E., Cornelissen, G., & Bachmann, R.T. (2015). Designing and performance evaluation of biochar production in a top-lit updraft upscaled gasifier, Journal of Sustainable Bioenergy System, 5, 41–55.